proceedings

Abstract

Passivation of MWIR heterostructure p-InAsSbP/n-InAs photodiodes using SiO_2 layers for near-room-temperature operation†

Jarosław Pawluczyk [1,*], Krzysztof Kłos [2], Oskar Ślęzak [3], Kinga Majkowycz [1], Krzysztof Murawski [1], Tetiana Manyk [1], Jarosław Rutkowski [1], and Piotr Martyniuk [1]

1 Institute of Applied Physics, Military University of Technology, ul. Kaliskiego 2, 00-908 Warsaw, Poland
2 Photin Sp. z o.o, ul. Lutosławskiego 15, 05-080 Klaudyn, Poland; kk@photin.eu
3 Vigo Photonics S.A., ul. Poznańska 129/133, 05-850 Ożarów Mazowiecki, Poland
* Correspondence: jaroslaw.pawluczyk@wat.edu.pl
† Not presented yet.

Abstract: We examined the effect of SiO_2 passivation on the parameters of mesa heterostructure InAs/InAsSbP photodiodes with a spectral responsivity 50% cut off at 3.5 µm at 295 K, specific to the InAs absorber layer. The R_0A product was found to increase by 30% after passivation of the devices of 113 µm in diameter, up to 0.9 Ωcm², while for those with a diameter of 1.13 mm, R_0A of 2.2 Ωcm² was achieved, with a value of $D^* > 3\times10^9$ cmHz$^{1/2}$/W at the peak of the spectrum, 1 kHz, 0 V bias, 295 K. To the best of our knowledge, this is the highest R_0A value at room temperature reported to date for a photodiode with an InAs absorber.

Keywords: Sensors, Indium arsenide, Photodiodes, Infrared detectors, Dark current

Citation: To be added by editorial staff during production.

Academic Editor: Firstname Lastname

Published: date

1. Introduction

Although MWIR spectral region (3–5 µm, medium wavelength infrared radiation) can be covered by different IV-VI and II-VI photodetectors (e.g. based on PbS, PbSe, HgCdTe), InAs photodiodes (PDs) appear to be the best choice for MWIR detection, due to mature technology of low-cost InAs substrates. The main advantage of InAs PDs is their ability to operate at near room temperatures. The elimination of cryogenic cooling reduces cost and results in more reliable operation. InAs photodiodes exhibit excellent noise characteristics at low frequencies and a fast response for detecting rapid processes. Compared to II-VI and IV-VI infrared detectors, InAs photodiodes demonstrate greater parameter stability [1]. However, at room temperature, the shunt resistance of the InAs photodiode is relatively low, comparable to the series resistance, which affects its responsivity [2] (389–391), [3]. Consequently, uncooled InAs photodetectors do not achieve background-limited performance. This effect is less pronounced in small-area detectors, which have higher shunt resistance and a lower surface area. Their performance can also be optimized by operating at lower temperatures achievable with thermoelectric mini-coolers. However, the contribution of surface leakage to dark current increases with cooling and decreasing diode area. Therefore, the development of fabrication and surface passivation technologies is currently prioritized to obtain bulk-limited leakage and achieve the specific detectivity attainable with the InAs compound. This is especially important when mesa structure chip processing is used, as is often the case in dense detector arrays. Etching that isolates the detector mesa structure disrupts the semiconductor crystal structure on mesa side walls, leaving there dangling chemical bonds that introduce surface states within the bandgap, pinning the surface Fermi level near the mid-gap. This causes non-zero surface potential and band-bending that forms a space-charge region at the side-wall, induces near-surface conductive leakage channels where accumulation of majority carriers or their inversion occurs, and facilitates Shockley-Read-Hall generation-recombination (GR), trap-assisted tunneling (TAT) and inter-band tunneling surface currents. The dangling bonds, native oxides and impurities on the surface create the additional surface states within the bandgap and the fixed surface charge that modifies band-bending and the related effects. The exposed to ambient atmosphere InAs reacts with atmospheric oxygen, forming indium oxide with elemental arsenic distributed through the oxide. Native oxides should therefore be avoided and removed from the InAs surface before its passivation. The wide-gap unipolar barrier suppresses the GR current generated at the surface edge and within the volume of the p-n junction. However, surface TAT through the barrier remains possible [4], along with GR induced by surface band-bending. Therefore, surface passivation of barrier detector mesa structures is necessary too. An ideal surface would be a wide-gap insulator, repelling carriers to active volume of the device, having negligible density of fixed charge and surface states.

InAs photodiodes operating at zero bias with a useful sensitivity, preferably without cooling, are desired for DC, low-frequency, low-power applications, in the laser-diode spectroscopy, laser range finding, medicine and environmental monitoring.

2. Materials and methods

The material composition of the device, doping, and thickness of the respective layers are given in the device cross-section diagram in Figure 1. The MWIR absorption region (absorber) of the photodetector (layer 2) is placed between the wide-gap unipolar barrier layer—the top contact for holes—and the heavily n-type doped bottom contact for electrons. The absorber is InAs layer 1.5 µm thick with unintentional n-type doping 1–3×10^{16} cm^{-3}. The barrier in the conduction band within the contact for holes blocks injection of electrons into the absorber. The highly degenerate n-type layer of the contact for electrons has very few holes so their injection into the absorber is reduced too. Thus, the dark current is minimized.

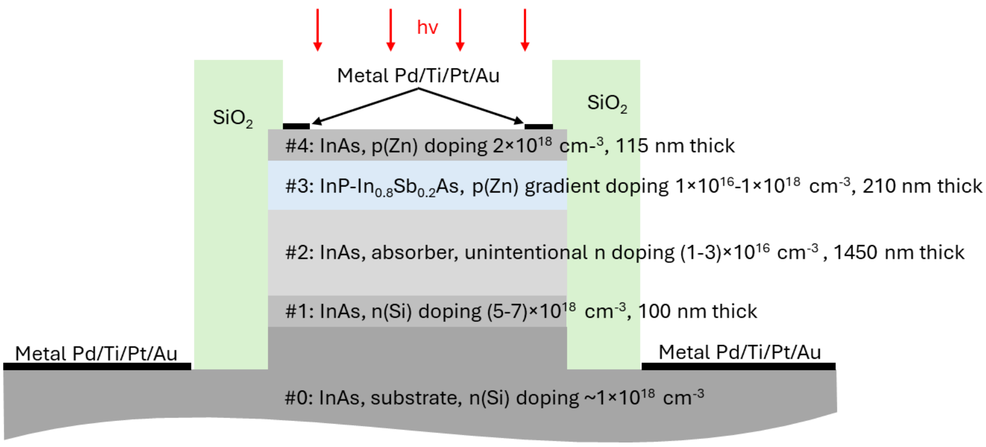

Figure 1. Diode cross-section diagram.

The detector structure was designed using Crosslight Software's SimuApsys software, a commercially available 2D/3D finite element analysis and modeling tool, which is particularly useful for simulating bulk semiconductor heterostructures. It solves the Poisson equation and the continuity equations, taking into account dependence of mobility on electric field, tunneling, avalanche multiplication, trap assisted mechanisms of carrier generation-recombination, heat transfer, material parameters dependent on temperature, optical phenomena (absorption, reflection, interference) and other factors. The package is equipped with a material database with data source references.

The device was grown, according to its design, in a horizontal MOVPE reactor at 50 hPa total pressure. The substrate used for the grown material was an Si-doped InAs epi-ready 2″ wafer, with n-type doping 1.5×10^{18} cm^{-3}, (100) oriented without deliberate surface miscut. The epitaxial growth began with a 100 nm thick n-doped InAs lower contact layer (#1 in Fig. 1), followed by the next layers as illustrated in Figure 1.

The as-grown multilayer films were characterized using optical microscopy, high-resolution X-ray diffraction, photoluminescence, and secondary ion mass spectrometry. The barrier layer showed properties of self-organized natural superlattices [5].

The passivation layer was SiO_2, grown by Inductively Coupled Plasma Chemical Vapor Deposition. A lower surface leakage and a higher R_0A were observed with a SiO_2 thickness of 50 nm compared to 500 nm. Particular attention was paid to removing photoresist and byproduct residues after both dry and wet etching steps to reduce the risk of increased surface leakage current.

The surface component of the dark current was estimated using Variable Area Diode Array test structures, using the following approximation [6]:

$$\frac{1}{R_0A} = \frac{1}{(R_0A)_V} + \frac{\alpha}{D} \quad (1)$$

where $(R_0A)_V$ approximates the R_0A product of an infinite area diode, D is the diode transverse linear size—diameter of the circular mesa, and α is a coefficient related to the surface generation of carriers at the diode perimeter.

3. Results

Figure 2 illustrates R_0A and DC dark current as a function of bias for the uncooled samples, showing reduced dark current and enhanced R_0A following passivation, for the best diodes across their respective size groups, ranging from the smallest (D = 113 μm) to the largest (D = 1128 μm), with the most significant improvement seen for the smallest devices. However, a several-fold variation in the measured dark current was noted within individual diode groups of a given size, including the forty-three smallest diodes. Additionally, the linear correlation between R_0A and size D disappeared when the same devices were measured at 215 K.

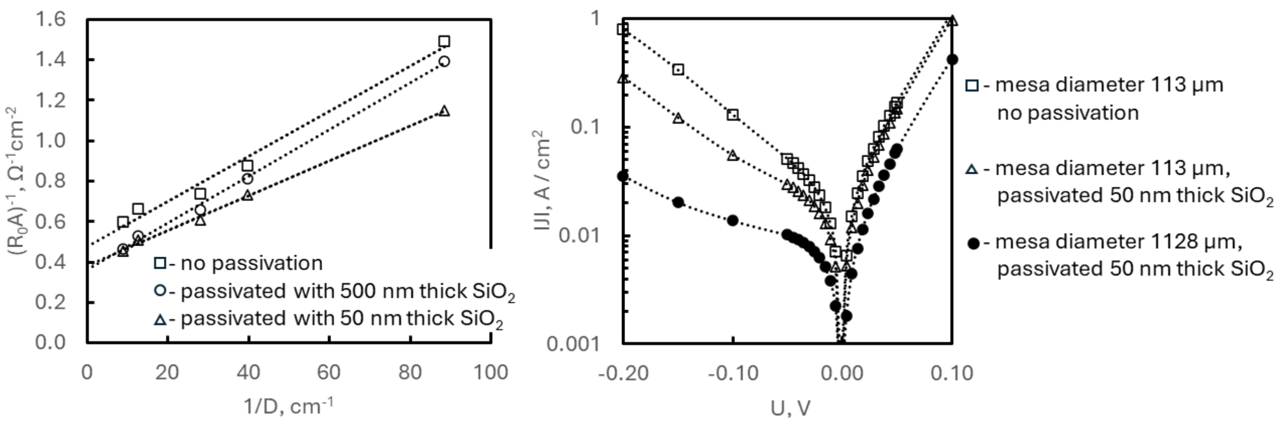

(**a**) (**b**)

Figure 2. Variable Area Diode Array sample measurement results at 295 K: (**a**) Reciprocal of R_0A product vs reciprocal of mesa structure transverse size D; (**b**) Absolute value of dark current density vs bias for the smallest and largest size.

4. Conclusions

The loss of correlation between diode size and the measured R_0A and dark current at 215 K may result from the dominance of surface carrier generation over volume generation at this temperature, as well as the observed variation in dark current intensity. This suggests that chip-processing technology, particularly cleaning procedures, still requires further optimization.

The obtained detector performance, also taking into account the measured spectral responsivity, surpasses that of commercially available InAs photodiodes [3, 7, 8]. To the best of our knowledge, we have produced uncooled InAs detectors with the highest R_0A value ever reported—even for barrier InAs diodes [9].

Author Contributions: Conceptualization, J.P., K.K. and P.M.; methodology, J.P.; K.K. and P.M.; software, T.M. and J.R.; validation, J.P., K.K., O.S., K.M. (Krzysztof Murawski) and K.M. (Kinga Majkowycz); formal analysis, J.P., K.K; K.M. (Krzysztof Murawski), K.M. (Kinga Majkowycz); investigation, J.P., K.K., J.R. and T.M.; resources, P.M. and J.P.; data curation, J.P., K.K., O.S., K.M. (Krzysztof Murawski) and K.M. (Kinga Majkowycz); writing—original draft preparation, J.P.; writing—review and editing, J.P., K.K., O.S., K.M. (Krzysztof Murawski), K.M. (Kinga Majkowycz), J.R. and P.M.; visualization, J.P., K.K., O.S., K.M. (Krzysztof Murawski), K.M. (Kinga Majkowycz) and J.R.; supervision, J.P., K.K., J.R. and P.M.; project administration, P.M.; funding acquisition, P.M. All authors have read and agreed to the published version of the manuscript.

Funding: This research was funded by the National Center for Research and Development (Poland), grant no. INNOGLOBO/II/65/PfBaAIRD/2023.

Institutional Review Board Statement: Not applicable.

Informed Consent Statement: Not applicable.

Data Availability Statement: Data are contained within the article.

Conflicts of Interest: The authors declare no conflicts of interest.

References

1. Tetyorkin, V.; Sukach, A.; Tkachuk, A. InAs Infrared Photodiodes. *Advances in Photodiodes* **2011**, 427-446. DOI: Book_Doi 10.5772/588.
2. Rogalski, A. *Infrared and terahertz detectors*; CRC press, 2019.
3. Indium Arsenide Detectors. Teledyne Judson Technologies, Ed.; 2025.
4. Du, X.; Savich, G. R.; Marozas, B. T.; Wicks, G. W. Suppression of Lateral Diffusion and Surface Leakage Currents in nBn Photodetectors Using an Inverted Design. *Journal of Electronic Materials* **2018**, *47* (2), 1038-1044. DOI: 10.1007/s11664-017-5753-9.
5. Wang, C. A.; Vineis, C. J.; Calawa, D. R. Self-organized vertical superlattices in epitaxial GaInAsSb. *Applied Physics Letters* **2004**, *85* (4), 594-596. DOI: 10.1063/1.1773368.
6. Srivastav, V.; Saini, N. K.; Sareen, L.; Bhan, R. K.; Sharma, R. K. Modeling Current Voltage Characteristics of MWIR HgCdTe Diodes at High Reverse Bias Voltage. *Environ Sci Eng* **2014**, 881-883.
7. InAs photovoltaic detectors. Hamamatsu Photonics K.K., S. S. D., Ed.; 2025.
8. InAs room-temperature photovoltaic infrared detectors. Vigo Photonics S.A., Ed.; 2025.
9. Savich, G. R.; Pedrazzani, J. R.; Sidor, D. E.; Maimon, S.; Wicks, G. W. Dark current filtering in unipolar barrier infrared detectors. *Applied Physics Letters* **2011**, *99* (12), 121112. DOI: 10.1063/1.3643515.